32nd International Conference
ENGINEERING MECHANICS 2026
Medlov, Czech Republic, May 11 – 13, 2026

BONE REMODELLING AROUND IMPLANT – TIME EFFECTIVE ALGORITHM

Votava T.[1], Marcián P.[2], Košková O.[3], Fuis V.[4], Wolff J.[5]

Abstract: *Numerical simulation of bone remodelling around implants is computationally demanding, especially for models based on high-resolution micro-CT data. Traditional approaches either reduce model resolution, which limits accuracy at the microstructural level, or employ voxel-based models that significantly increase computational cost due to stress concentration effects. This study presents a hybrid computational approach that combines an irregular finite element mesh for stress–strain analysis with a regular mesh for efficient stimulus calculation. Stress and strain energy density values are transferred between the two domains using transformation matrices. Bone remodelling is simulated using the adapted Huiskes–Weinans. The method was demonstrated on a two-dimensional model of trabecular and cortical bone surrounding a cranial fixator screw. Results show that the proposed approach significantly reduces computational time while preserving biologically relevant stimulus evaluation and expected remodelling behaviour. The method provides an efficient and accurate alternative for large-scale bone remodelling simulations.*

Keywords: Bone remodelling, Implant, FFT, Micro-CT

1. Introduction

Solving bone modelling/remodelling simulations around an implant using Finite element method (FEM) is a time-consuming issue. Bone remodelling process is described by a differential equation, which is solved in a discretized form using an iterative method. To obtain the final state, thousands of iterations must be performed. For large computational models, especially those based on micro-CT data, this may require months of computation (due to large number of nodes).

There are several ways to reduce computational time. One option is to decrease the resolution of the computational model, which is typically derived from CT images. Although this approach cannot capture the final distribution at the microstructural level, it significantly reduces the time required to solve the stress–strain state. However, this simplification complicates bone remodelling simulations. The mechanical stimulus, defined as a weighted sum of strain energy density sensed by osteocytes (Weinans 1992), is evaluated at computational nodes that generally do not coincide with the actual locations of osteocytes. As a result, stimulus evaluation becomes more complex and may lead to increased computational time.

[1] Ing. Tomáš Votava, Dis.: Institute of Solid Mechanics, Mechatronics and Biomechanics, Brno University of Technology, Technická 2896/2; 616 69, Brno; CZ, 200956@vutbr.cz

[2] Ing. Petr Marcián, PhD.: Institute of Solid Mechanics, Mechatronics and Biomechanics, Brno University of Technology, Technická 2896/2; 616 69, Brno; CZ, macian@fme.vutbr.cz

[3] Olga Košková, MD, PhD, Department of Burns and Plastic Surgery, University Hospital Brno and Faculty of Medicine, Masaryk university, Jihlavská 20, 625 00, Brno; CZ, koskova.olga@fnbrno.cz

[4] Assoc. Prof. Vladimír Fuis, PhD.: Centre of Mechatronics – Institute of Thermomechanics of the Czech Academy of Sciences – branch Brno and Faculty of Mechanical Engineering, Brno University of Technology, Technická 2896/2; 616 69, Brno; CZ, fuis@fme.vutbr.cz

[5] Prof. Jan Wolff, PhD Klinik für Kiefer- und Gesichtschirurgie, Campus Lübeck, Ratzeburger Allee 160/Haus D3, 23538 Lübeck, Germany, Jan.Wolff@uksh.de

ISSN: 1805-8256, doi: 10.21495/em2026-149

Another option is to use a voxelized computational model. However, the stair-step approximation of the geometry inherent to voxel-based models introduces sharp geometric discontinuities at voxel boundaries, leading to stress singularities. Consequently, small element and voxel sizes are required to mitigate these artificial singularities, which again results in increased computational time.

Both approaches have advantages and disadvantages, as described above. The idea of this study is to combine these two approaches. For solving stress strain states irregular mesh (obtained from segmented CT or micro-CT) was used. Strain energy density from irregular mesh was transformed using interpolation to regular mesh to calculate stimulus. Stimulus is than transformed with inverse function to irregular mesh where bone density increment via nodes was calculated.

2. Methods

For simulation micro-CT image from *os occipitale* was used. The solution was divided into two domains. The first domain consists of a finite element mesh, which is used to solve the stress–strain states. The second domain is a regular mesh used for stimulus calculation. The workflow of the bone remodelling simulation is shown in Fig. 1.

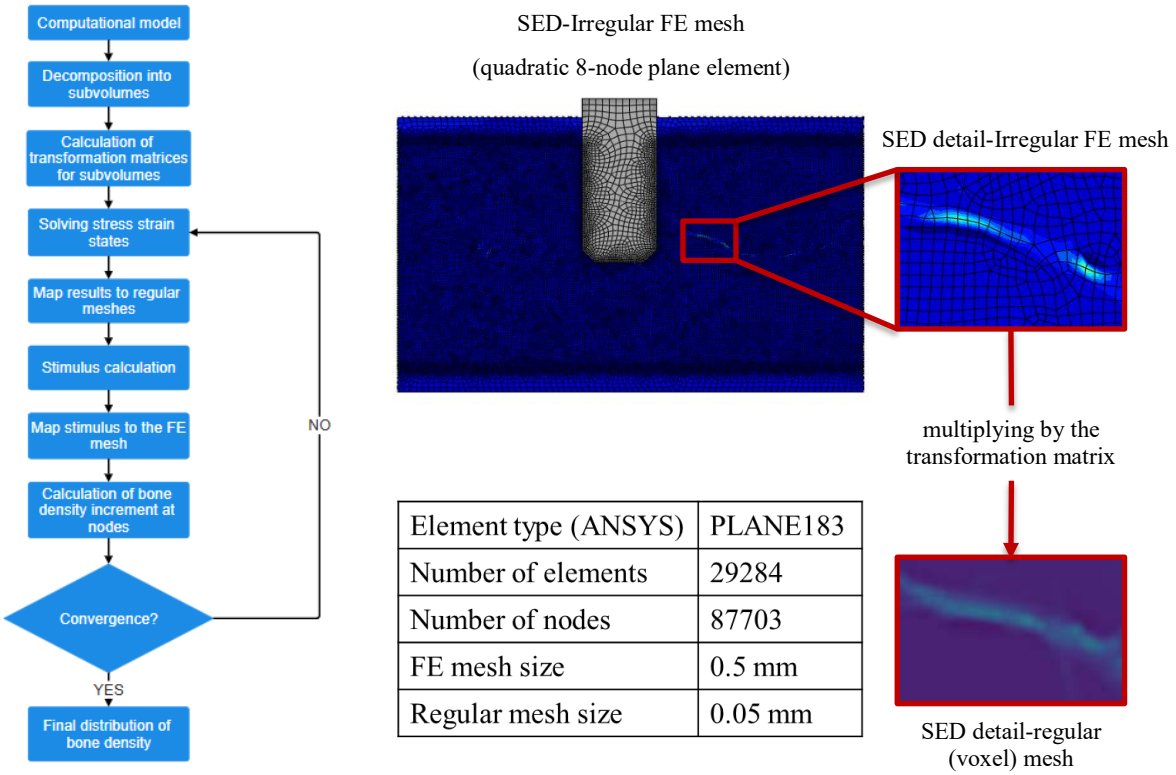

Element type (ANSYS)	PLANE183
Number of elements	29284
Number of nodes	87703
FE mesh size	0.5 mm
Regular mesh size	0.05 mm

Fig. 1: Bone remodelling flowchart (left) and demonstration of interpolated SED values (right).

For solving stress strain states software Ansys (ANSYS Academic Research Mechanical, Release 23.2; Swanson Analysis Systems Inc) was used. The finite element mesh can be divided into smaller subvolumes, which reduces the computation time required for the transformation matrices. The resolution of the regular mesh should be equal to or greater than the mean osteocyte distance. At the same time, the resolution of the regular mesh should at least correspond to the resolution of the CT images used for segmentation. Values in the regular mesh elements are obtained by interpolation of nearby values from the irregular finite element mesh. The relationships between quantities in the finite element mesh and the regular mesh are represented by transformation matrices.

2.1. Model of geometry

For testing purposes, a two-dimensional analysis of remodelling around a cranial fixator screw was performed. The geometric model consists of trabecular bone, cortical bone, and the screw (Fig. 2). The trabecular bone was created by segmentation of micro-CT images (voxel size 25 µm × 25 µm × 25 µm). The cortical bone and the screw were additionally modelled using CAD software. Their representation is

schematic only: the cortical bone has a uniform thickness, and the screw is modelled without threads. For discretization quadratic 8-node node plane element (in Ansys PLANE183) was used. The finite element mesh is available at the link: 10.5281/zenodo.19550154.

2.2. Boundary conditions

The computational model is fixed on both sides. To simulate typical loading conditions of the screw, a force perpendicular to the axial direction of the screw was applied (Fig. 2). The force magnitude was set to 100 N, as the analysis is qualitative and the main purpose of the simulation is to test the proposed

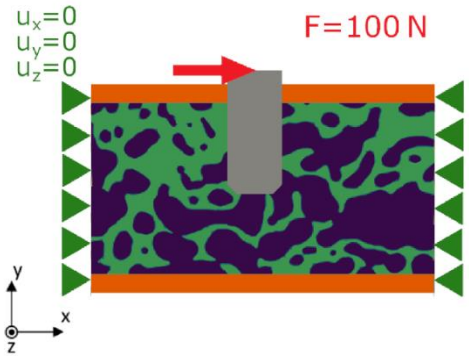

Fig. 2: Model of geometry and boundary condition.

method.

2.3. Model of material

For the purposes of this study, the implant, trabecular bone, and cortical bone were assumed to be homogeneous, isotropic, and linearly elastic materials. The implant material is characterized by a Young's modulus of $E = 110$ GPa and a Poisson's ratio of $\mu = 0.3$ [–]. Cortical bone is represented by a Young's modulus of $E = 15$ GPa and a Poisson's ratio of $\mu = 0.3$ [–] (Rho, 1993). The Young's modulus of trabecular bone is assumed to be dependent on bone density according to the following relationship (Marcián, 2021):

$$E = 13.636\left(\frac{1000\cdot\rho+3295.6}{0.221}\cdot 2.11\cdot 10^{-4} - 3.3\right) \text{[GPa]} \quad (1)$$

where $\rho\ \left[\frac{g}{cm^3}\right]$ is bone density. The Poisson's ratio of trabecular bone was assumed to be a constant value of μ*=0.3 [-]* (Rho 1993).

2.4. Bone remodelling algorithm

The strain energy density (SED) at the nodes of the finite element mesh is multiplied by a transformation matrix to obtain interpolated values on the regular grid. For micro-level remodelling simulations, the Huiskes–Weinans algorithm (Weinans, 1992) was adopted, with mechanical stimulus, defined as:

$$P(\mathrm{x}) = \sum_{i=1}^{n} U_i \cdot \exp\left(-\frac{d(\mathrm{x})}{d_0}\right) \quad (2)$$

where U_i is the strain energy density of each sensor cell, d is the distance of the sensor cell from the actor cell and $d_0 = 0.1\ mm$ (Isaakson 2009) is the distance from the sensor cell for which the stimulus is reduced to 37%. This equation represents a discrete form of convolution that is easy to compute on a regular mesh. To ensure bone growth only at the interface between bone tissue and the intertrabecular space, the matrix representing the regular mesh was multiplied by a mask matrix representing trabecular bone and dilated. The stimulus in the regular mesh was then multiplied by the inverse transformation matrix to obtain the stimulus at the nodes of the finite element mesh, which was subsequently used to calculate the bone density increment according to the following equation:

$$\frac{\Delta\rho}{\Delta t} = \begin{cases} A(P(\mathrm{x}) - U_{ref}(1+s)) & \text{if } P(\mathrm{x}) \geq U_{ref}(1+s) \\ 0 & \text{if } U_{ref}(1-s) < P(\mathrm{x}) < U_{ref}(1+s) \\ A(P(\mathrm{x}) - U_{ref}(1-s)) & \text{if } P(\mathrm{x}) \leq U_{ref}(1+s) \end{cases} \quad (3)$$

where U_{ref} is the reference stimulus, s is the remodeling equilibrium zone half-width and A is a time constant. Since analysis is qualitative U_{ref} and A were obtained through sensitivity analysis.

3. Results

For demonstration purposes, 1000 iterations were performed. Final distribution after 1000 iteration is shown in Fig. 3.

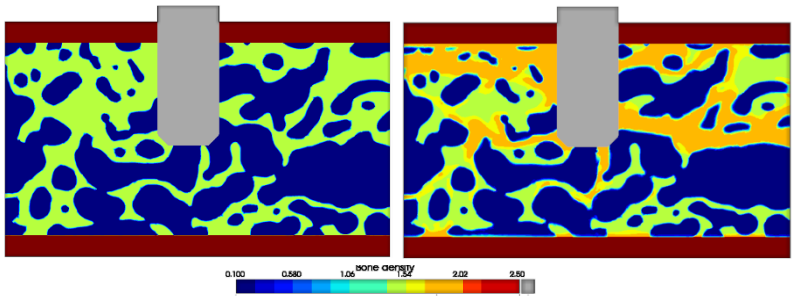

Fig. 3: Initial (left picture) and final distribution (right picture) of bone density.

In Fig. 4 is demonstrated initial border of bone tissue – bone marrow interface mapped on final distribution. In detail is evident that expected behaviour including changes in bone density and trabecular thickness was achieved.

4. Discussion

From Fig. 3 it is evident that the trabecular interface is not as smooth as expected. This is caused by irregularities in the finite element mesh, which represent the main disadvantage of the proposed approach. Another limitation is the interpolation itself: in the case of a coarse finite element mesh, peak SED values may not be captured, and interpolation cannot compensate for this error.

The advantage of this method is precise stimulus calculation. For irregular meshes, the stimulus in the presented form (a weighted sum of SED from osteocytes within a given area) is a challenging problem; moreover, the more irregular the mesh, the less accurate the resulting sum becomes. This indicates that the proposed approach better respects the underlying biological behaviour of bone tissue.

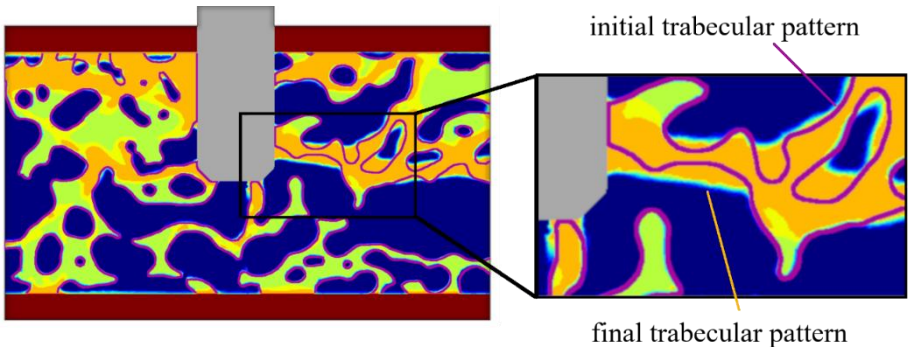

Fig. 4: Final distribution of bone density with initial bone tissue/marrow interface.

Acknowledgement

This publication was supported by the project "Mechanical Engineering of Biological and Bio-inspired Systems", funded as project No. CZ.02.01.01/00/22_008/0004634 by Programme Johannes Amos Commenius, call Excellent Research. The research was supported by the specific research FSI-S-26-8981 and institutional support RVO: 61388998.

References

Marcián, P. et al., 2021. On the limits of finite element models created from (micro)CT datasets and used in studies of bone-implant-related biomechanical problems. *Journal of the Mechanical Behavior of Biomedical Materials*, 117(5), p.104393.

Isaksson, H. et al., 2008. Remodeling of fracture callus in mice is consistent with mechanical loading and bone remodeling theory. *Journal of Orthopaedic Research*, 27(5), pp.664-672.

Rho, J.Y., Ashman, R.B. & Turner, C.H., 1993. Young's modulus of trabecular and cortical bone material: Ultrasonic and microtensile measurements. *Journal of Biomechanics*, 26(2), pp.111-119.

Weinans, H., Huiskes, R. & Grootenboer, H.J., 1992. The behavior of adaptive bone-remodeling simulation models. *Journal of Biomechanics*, 25(12), pp.1425-1441.